Forming Patterned Films with Tethered Diblock Copolymers

Ekaterina B. Zhulina,[†] Chandralekha Singh,[†,‡] and Anna C. Balazs*[,†]

Materials Science and Engineering Department and Physics and Astronomy Department, University of Pittsburgh, Pittsburgh, Pennsylvania 15261

Received April 2, 1996; Revised Manuscript Received June 28, 1996[⊗]

ABSTRACT: We use self-consistent-field calculations and scaling arguments to determine the behavior of AB diblock copolymers that are tethered to a surface. While the surrounding solution is assumed to be a poor solvent for both components, the B block is considered to be less soluble than the A. The solvophobic interactions within the system drive the chains to self-assemble into micelles that have an "onion-" or "garliclike" structure. The specific morphology and dimensions of the micelles depend on the relative block lengths and whether the chains are grafted by the more or the less soluble component. At sparse grafting densities, the layer contains an ordered array of such micellar structures and the film forms a distinct pattern. The size and spacing of the patterns can be manipulated by varying the molecular weights of the copolymers. Thus, the results provide guidelines for fabricating well-defined patterned films.

Introduction

One means of forming patterned polymer films is to tether the ends of the chains onto a substrate and immerse the system in a poor solvent. The solvophobic interactions drive the chains to phase separate, but since the ends are immobile, the polymers can only microphase separate into finite domains. For example, in poor solvents tethered homopolymers associate into pinned micelles on the surface. If the grafting is roughly uniform, the polymers form an ordered array of such micelles,[1−3] and the layer exhibits a distinct pattern.[4] Recently, we exploited the incompatibility between solvent and tethered chains to create patterned films with two homopolymer-coated surfaces[5,6] and with copolymers.[7] In the former case, we first considered two parallel layers of end-grafted homopolymers.[5] As the layers are compressed, the pinned micelles from the two surfaces merge, forming a larger micelle or "bundle", which extends from one surface to the other. In this way, the layers form a film with well-defined corrugations. In addition, we examined the behavior of bridging homopolymers, where one end of each chain is tethered to one surface and the other end is tethered to the second parallel surface.[6,8] This system also exhibits novel patterns as a function of surface separation. For a finite range of surface separations, the polymers form pinned micelles that are preferentially located on either of the surfaces. As the surface separation is increased, the micelles become localized in the middle of the gap. Now, the film is decorated with pinned micelles in the center of the layer. For long chains, this transition from "surface-to-center" is sharp and resembles a first-order phase transition.[6]

In the case of copolymers, one can vary not only the solvent affinities of each component but also the interaction energy between the different monomers. Consequently, the system can be driven to form more complicated patterns than may be possible with homopolymers.[7,9−11] For example, we recently determined the phase behavior of tethered Y-shaped AB copolymers, where one arm of the Y is an A copolymer and the other is a B chain.[7] When the Flory−Huggins interaction parameter between the A and B chains, χ_{AB}, is approximately zero and the chains are immersed in a poor solvent, the copolymers form pinned micelles similar to those formed by homopolymers. Introducing an effective A−B repulsion (by setting $\chi_{AB} > 0$), however, causes significant structural changes. In particular, each micelle splits into two, forming one micelle of pure A and another of pure B. Within the grafted layer, the chains rearrange so that A blocks associate with neighboring A's and the B blocks aggregate with neighboring B's. In effect, the layer now self-assembles into a checkerboard pattern.

In this paper, we continue our studies on forming patterned films by considering the poor solvent behavior of linear, AB diblock copolymers that are grafted by one end onto a planar surface. As indicated by our previous study of tethered copolymers,[7] the chemical linkage between the different blocks will give rise to novel structures. In effect, this behavior is in direct analogy with the microphase separation of diblocks in the melt. Here, we primarily focus on the situation where χ_{AB} is close to zero, but the solvent affinities of the different blocks are significantly different. Under these conditions, the polymer−solvent interactions will govern the formation of supramolecular structures within the grafted layer. We use both self-consistent-field (SCF) calculations and scaling arguments to characterize the features of these structures. With the SCF model, we demonstrate the formation of novel types of pinned micelles: "onions" and "garlics", where the less soluble blocks form the inner core and the more soluble fragments form an outer coating. Through scaling theory, we determine how the size and shape of these structures vary with the solvent quality and the properties of the diblocks. We also determine a phase diagram that delineates where these different structures appear as a function of the relevant parameters.

The paper is organized as follows. We start with a description of the system under consideration and then proceed with a brief summary of the SCF approach. We then describe the results of our calculations for grafted diblock copolymers. On the basis of the semiquantitative picture obtained from the SCF method, we develop a "blob" model of the system and determine scaling laws for these structures. Finally, we summarize our conclusions from these studies.

[†] Materials and Science and Engineering Department.
[‡] Physics and Astronomy Department.
[⊗] Abstract published in *Advance ACS Abstracts,* August 15, 1996.

S0024-9297(96)00498-6 CCC: $12.00 © 1996 American Chemical Society

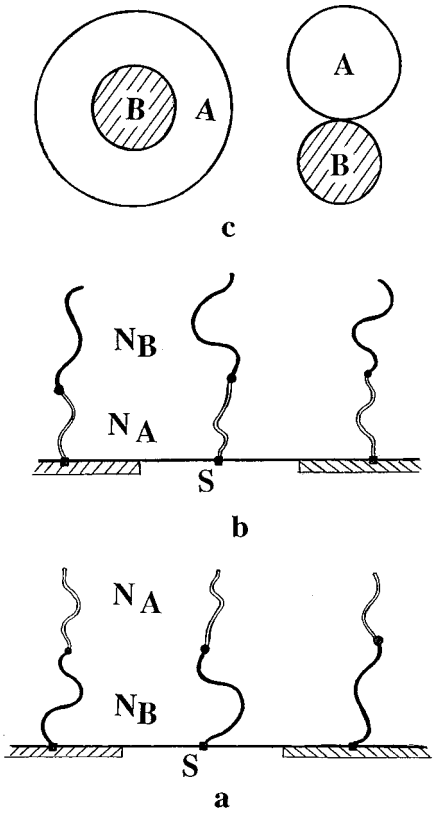

Figure 1. Schematic diagram of (a) chains tethered by the less soluble B block, (b) the diblock chains grafted onto the surface by the more soluble A block, and (c) "onion" and "dumbbell" conformations for a single chain. The parameter s marks the area per chain.

The System

We consider flexible AB diblock copolymers that are grafted onto a flat surface. The grafting density is given by $1/s$, where s is the area per chain. The blocks contain $N_A \gg 1$ and $N_B \gg 1$ symmetrical units of size a (see Figure 1). The layer is immersed in a solution that is a poor solvent for both components; thus, both solubility parameters are positive in value: $\tau_A = (\Theta_A - T)/T > 0$ and $\tau_B = (\Theta_B - T)/T > 0$. Here, Θ_A and Θ_B are the corresponding theta temperatures for the components of the diblock. Thus, the values of the second virial coefficients, $v_A \sim -a^3\tau_A$ and $v_B \sim -a^3\tau_B$ are negative, implying that contacts between like monomers are attractive. The third virial coefficients w_A and w_B are assumed to be positive (ternary contacts are repulsive) and close to unity for both components. We also assume that the value of χ_{AB}, the Flory–Huggins interaction parameter between the A and B monomers, is close to zero (the blocks are nearly compatible), and the interaction of the blocks with the surface is the same as that with the solvent. Thus, all interactions in the system are described by the two parameters, $\tau_A = {}^1/_2 - \chi_{AS}$ and $\tau_B = {}^1/_2 - \chi_{AS}$, where χ_{AS} and χ_{BS} are the Flory–Huggins parameters for the respective polymer–solvent interactions. We focus on relatively sparse grafting densities, i.e., the case where pattern formation is known to be most pronounced.[1–4]

The Self-Consistent Field Model

The results from the SCF calculations provide a description of the system at thermodynamic equilibrium. One-dimensional SCF theory, however, is insufficient for describing laterally inhomogeneous structures, such as the pinned micelles. We therefore use a two-dimensional SCF theory, which is a generalization of the 1D model developed by Scheutjens and Fleer.[12] In the Scheutjens and Fleer theory, the phase behavior of polymer systems is modeled by combining Markov chain statistics with a mean-field approximation. Since the method is described thoroughly in ref 12, we simply provide the basic equations and refer the reader to that text for a more detailed discussion.

To start, the free energy per site in the mean field approximation is given by

$$f(r) = \sum_{i,c} n_{i,c}(r) \ln n_{i,c}(r) + {}^1/_2 \sum_{j,k} \chi_{j,k} \int \eta(r - r')\, \phi_j(r)\, \phi_k(r')\, dr' \quad (1)$$

where the first term on the right-hand side represents the entropy of mixing and the second term is the enthalpic contribution. The parameter $n_{i,c}(r)$ is the number density at r of molecules of type i in conformation c. In the enthalpic term, the indices j and k run over all the different types of segments and $\phi_j(r)$ represents the average density of monomers j at r. The $\chi_{j,k}$ term is the Flory–Huggins interaction parameter, and $\eta(r - r')$ is the short-range interaction function, which is replaced by a summation over nearest neighbors.

To calculate the segment density distribution $\phi_j(r)$ that minimizes the free energy, we exploit the analogy between the trajectory followed by a diffusing particle and the conformation of a chain.[12] We define Green's functions of the type $G(r_1,N'|r_2,N'')$ as the combined statistical weight of all conformations of a subchain starting with segment N' at r_1 and ending with segment N'' at r_2. For a homopolymer, the set of Green's functions for $N' < N''$ and $N' > N''$ are identical and obey the recursion relation

$$G(r,N'|r_1,1) = \exp[-U_i(r)] \int G(r',N' - 1|r_1,1)\, \eta(r - r')\, dr' \quad (2)$$

along with the boundary condition

$$G(r,1|r',1) = \exp[-U_i(r)]\, \delta(r - r') \quad (3)$$

where $\delta(r - r')$ is the Kronecker delta, and r and r' are the variables that denote the beginning and end of the chain, respectively. The parameter $U_i(r)$ is the potential of mean force acting on segment i at point r and is given by

$$U_i(r) = \alpha(r) + \sum_k \chi_{i,k} \int \phi_k(r')\, \eta(r - r')\, dr' \quad (4)$$

where $\alpha(r)$ is a hard-core potential that ensures incompressibility. The segment density distribution can be calculated from the Green's functions as

$$\phi_j(r) = \sum_i C_i \exp[-U_j(r)] \sum_{N' \in j} \int G(r,N'|r_1,1)\, G(r,N'|r_2,N_i)\, dr_1\, dr_2 \quad (5)$$

where N_i is the length of molecule i and C_i is the normalization constant, which can be obtained from the total number of molecules n_i:

$$C_i = n_i/[\sum_{N'} \int G(r_1,N'|r_2,1)\, dr_1\, dr_2] \qquad (6)$$

From eqs 2−6, the self-consistent density distribution for the different types of segments can be calculated by discretizing the equations and solving them numerically.[12] In the two-dimensional SCF theory, the above equations are written explicitly in terms of y and z, rather than r, and the mean-field approximation is applied along the x direction. (In other words, we assume translational invariance along the x direction. Nonetheless, the probability of having a neighbor in the x direction is included in the calculation of the Green's functions.)

In our calculations, the tethered diblocks are assumed to be monodisperse. The ends of the chains are grafted to the $z = 1$ plane, which represents the surface. The Green's function for the grafted segment i at the $z = 1$ surface can be written as $G_i(y,z) = \delta(y - y_i)\, \delta(z - 1)$. The chains are grafted at every alternate lattice site along the y direction. The parameter ρ gives the grafting density per line along x, the mean-field direction. (This implies that the average spacing between points along a line in x is $1/\rho$ and the area per chain is $s = 2/\rho$.) Periodic boundary conditions are applied along the y direction.

The values of the relevant parameters are given by $\rho = 0.025$, $\chi_{AB} = 0$, $\chi_{AS} = 1$, and $\chi_{BS} = 2$. Thus, the surrounding solution is a poor solvent for both blocks, but the B block is less soluble than the A segment. We consider how the morphology of the layer is effected by having the more or the less soluble block near the surface. Specifically, we examine the behavior of the film when the chains are anchored by the end of the less soluble B and when they are tethered by the end of the A fragment. In both studies, we systematically vary N_A and N_B to determine how the block length affects pattern formation.

Results from SCF Calculations

Chains Grafted by the Less Soluble Block. We first investigate the case where each chain is tethered by the end of the less soluble B component (see Figure 1a). We fix the length of the B block at $N_B = 80$ and gradually increase the length of the A component. The density profiles for the resulting self-assembled structures are shown in Figure 2. Frames a−c reveal that the block copolymers associate into "onion" structures, where the less soluble B's form the inner core and the more soluble A's form the outer layer. In this conformation, the encircling A's shield the B's from the unfavorable solvent and the surface tensions within the system are minimized. As frame (a) shows, this structure is favored even when N_A is relatively small (equal to 20).

As N_A is increased, the polymer density within the A shell also increases. With an enhancement in the outer layer, the B blocks are more effectively shielded from the energetically unfavorable solvent. When $N_A \sim 100$ (as in Figure 2c), the polymer density within the outer shell reaches a maximum value, it becomes comparable to the density within the core of a pinned micelle formed from grafted A homopolymers when $\chi_{AS} = 1$.[5] Thus, further increases in N_A do not alter the density of the outer shell but do enhance both the lateral and vertical extent of the A coating. Since the B blocks are now well shielded from the solvent, the dominant enthalpic losses arise from contacts between the outer A layer and the solvent. If N_A is increased further, the losses at the boundaries of the A layer become sufficiently large that two adjacent shells are driven to merge and thereby minimize their contact with the solvent. This merging into a common shell causes structural rearrangements of the B cores; the two cores, which are shielded by the same A layer, move closer together. Further increases in N_A can cause further merging of the outer A shells (see discussion in the Scaling Theory section below). Since the multiple cores are simultaneously shielded by a common A shell, the micelle resembles a "garliclike" structure, as seen in Figure 2d.

The number of chains in a micelle, f, increases very slowly as N_A is increased. The relative insensitivity of f to the length of the outer A block is due to the fact that f is mainly determined by the cost of stretching the "legs", the segments that tether the core to the surface. With $N_B = 80$, the legs are primarily formed from the grafted B blocks.

Finally, we note that with the increase in N_A, there is a small but gradual decrease in the relative amount of B within the spherical portion of the structure since the abundant A begins to dominate this region. Also, as N_A increases, the density of A near the surface increases while that of B decreases so that the latter is somewhat more extended in the Z direction (see Figures 2c,andd).

Chains Tethered by the More Soluble Block. We now determine what structures are formed when the chains are tethered by the ends of the more soluble A blocks (see Figure1b). Figure 3 allows us to visualize these structures and reveals the morphological changes that occur when N_A is gradually increased while N_B is held fixed at 80. When N_A is small (20 sites), each A block contributes to forming the legs of the micelles, whose cores are composed of the more solvent-incompatible B. As N_A is increased, the legs become less stretched and the A's again form an outer shell around the inner core to minimize the contact between the B's and the solvent. With further increases in N_A, the density of A around the poorer component gradually increases and thus becomes more effective in shielding the B's.

Since the A's are closer to the surface, increasing N_A causes the B core to be pushed away from the grafting surface in the vertical direction. In addition, less and less of the B's contribute to the legs of the micelle, and once N_A is sufficiently long, the legs are composed entirely of A (see Figure 3d).

Here, f is more sensitive to N_A than in the previous case, where the chains are anchored by the B blocks. This is not surprising, and for sufficiently large values of N_A, we expect that f will scale with N_A in the same manner as grafted A homopolymers (in poor solvents).

Comparison of Figures 2 and 3 reveals that for $N_B = 80$ and $N_A = 20$ or 40, the shielding of the B cores is more effective when the chains are tethered by the B's than when they are grafted by the A's. In the latter case, the grafted A blocks form the legs, and the stretching cost for shielding the B cores with short A blocks is higher than in Figure 2. Comparison of $N_B = 80$ and $N_A = 120$ in the two cases shows that the B cores are more extended in the Z direction in Figure 3 than in Figure 2 since the B chains are grafted in Figure 2 while they are free in Figure 3. Moreover, the size of the micelle in Figure 3d is larger than in Figure 2c because f is more affected by the value of N_A when the chains are tethered by the A block (as in Figure 3).

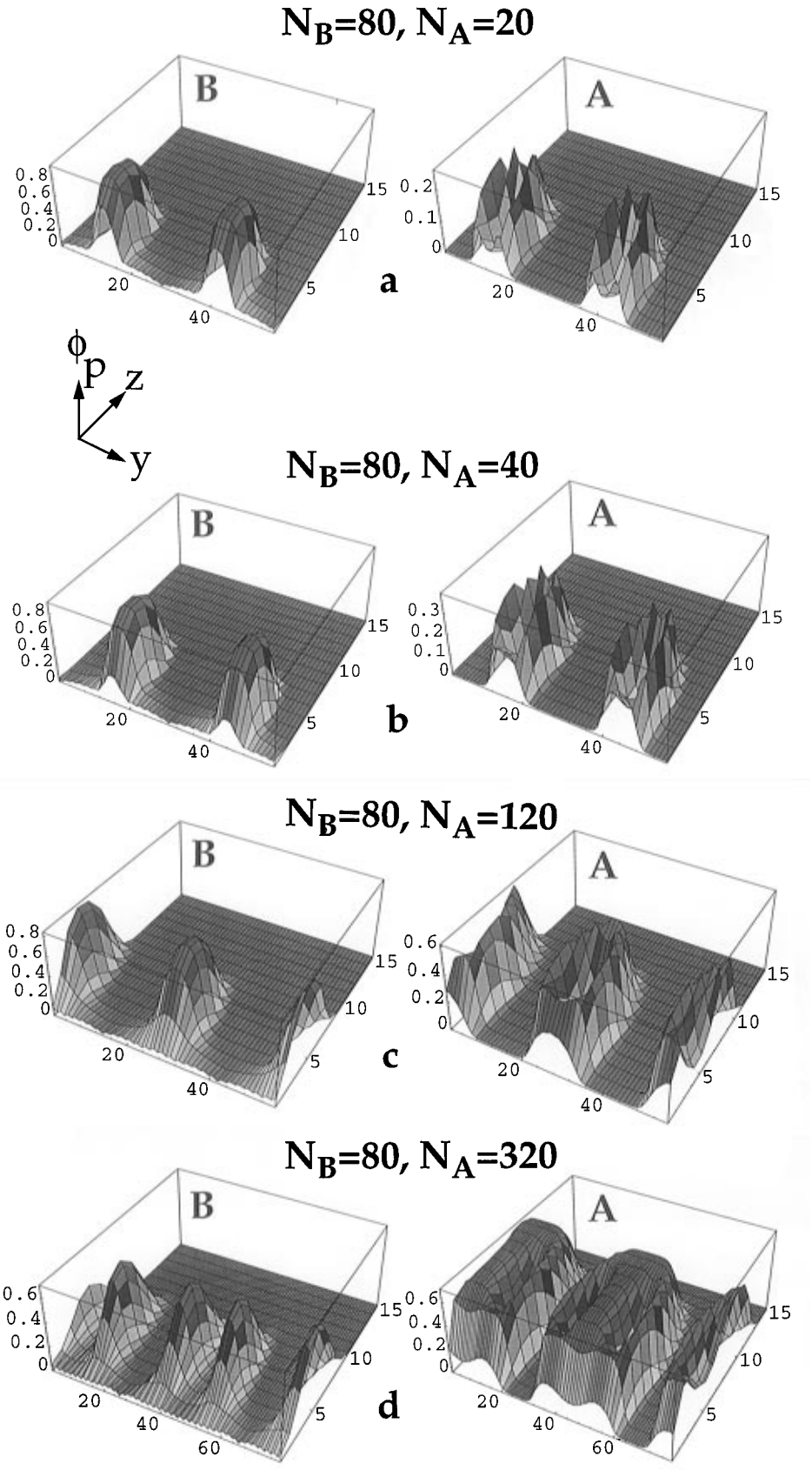

Figure 2. Results from the 2D SCF calculations. The plots reveal the effect of increasing N_A, while keeping N_B fixed at 80. The diblock copolymers are grafted by the less soluble B component. The parameter N_A has the following values: (a) $N_A = 20$, (b) $N_A = 40$, (c) $N_A = 120$, and (d) $N_A = 320$. Here, $\rho = 0.025$, $\chi_{Bs} = 2$, $\chi_{AS} = 1$, and $\chi_{AB} = 0$. Y refers to the grafting direction and ϕ_p denotes the polymer density. The plots marked B show the polymer density of the B blocks, while the plots marked A show the density of the A blocks.

Here, we also consider the changes that occur when N_A is held fixed at 80, while N_B is increased (see Figure 4). When N_B is very small (20 sites), the B's form a small core that is shielded in all directions by the A's. As N_B increases, the number of chains in the core and in the entire micelle increases; this causes an increase

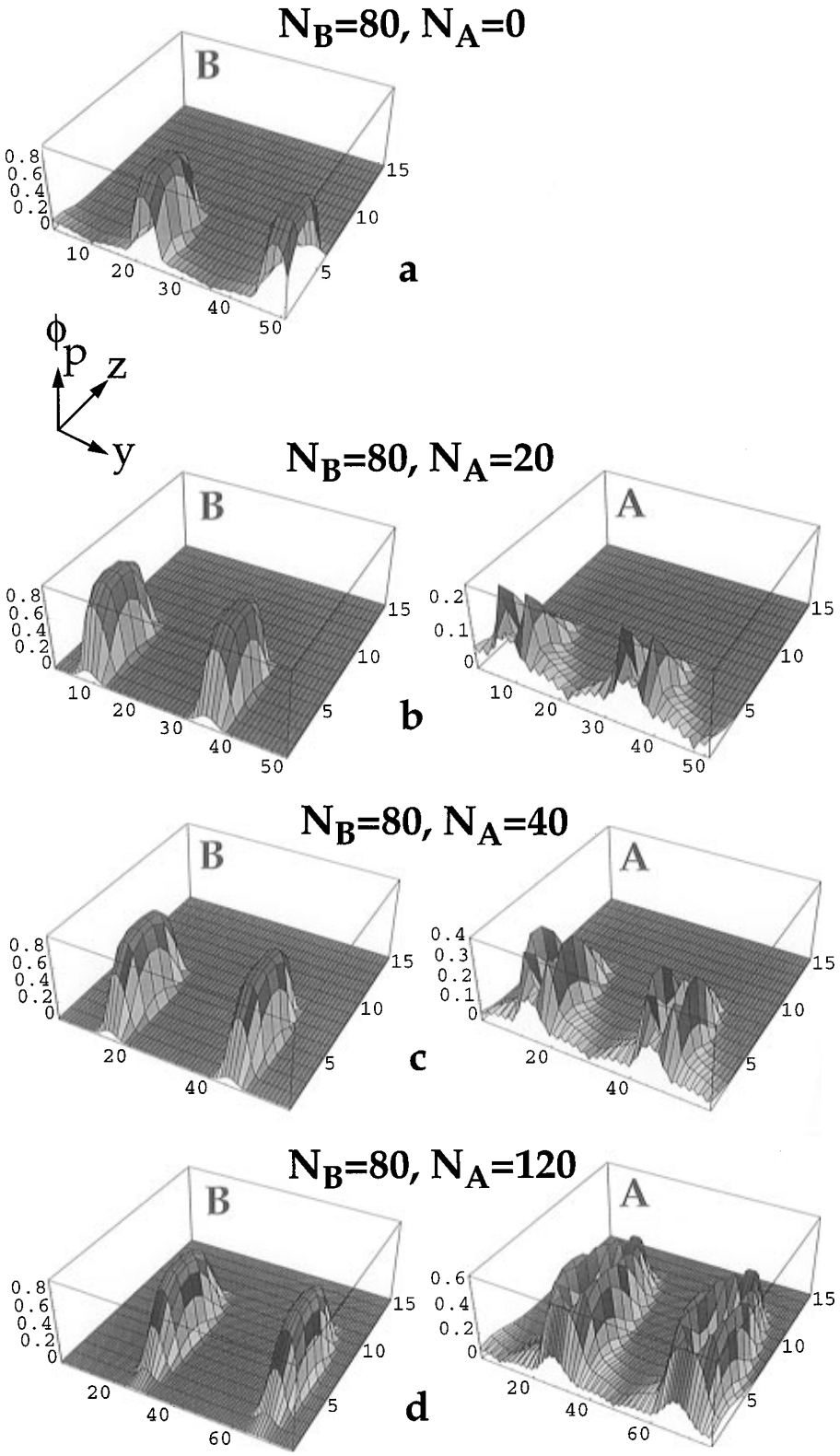

Figure 3. Results from the 2D SCF calculations. The plots reveal the effect of increasing N_A,while keeping N_B fixed at 80. The diblock copolymers are grafted by the more soluble A component. The parameter N_A has the following values: (a) $N_A = 0$, (b) $N_A = 20$, (c) $N_A = 40$, and (d) $N_A = 120$. The other parameters are set at $\rho = 0.025$, $\chi_{BS} = 2$, $\chi_{AS} = 1$, and $\chi_{AB} = 0$. Y refers to the grafting direction and ϕ_p denotes the polymer density. The plots marked B show the polymer density of the B blocks, while the plots marked A show the density of the A blocks.

in the size and extent of the micelle in the *Z* direction. The core remains surrounded by the more soluble component, giving the structure an "onion" appearance.

Although the density of the core initially increases with the length of B, once N_B is sufficiently long, the core density depends only on the value of χ_{BS} and becomes independent of N_B. (This phenomenon was also observed for grafted homopolymers,[5] where for sufficiently large chains, the core density depends only on the value of the polymer-solvent χ.)

As for the outer A shell, there is a small but gradual decrease in the density of A around the B core. This is due to the fact that N_A is held fixed and the shell

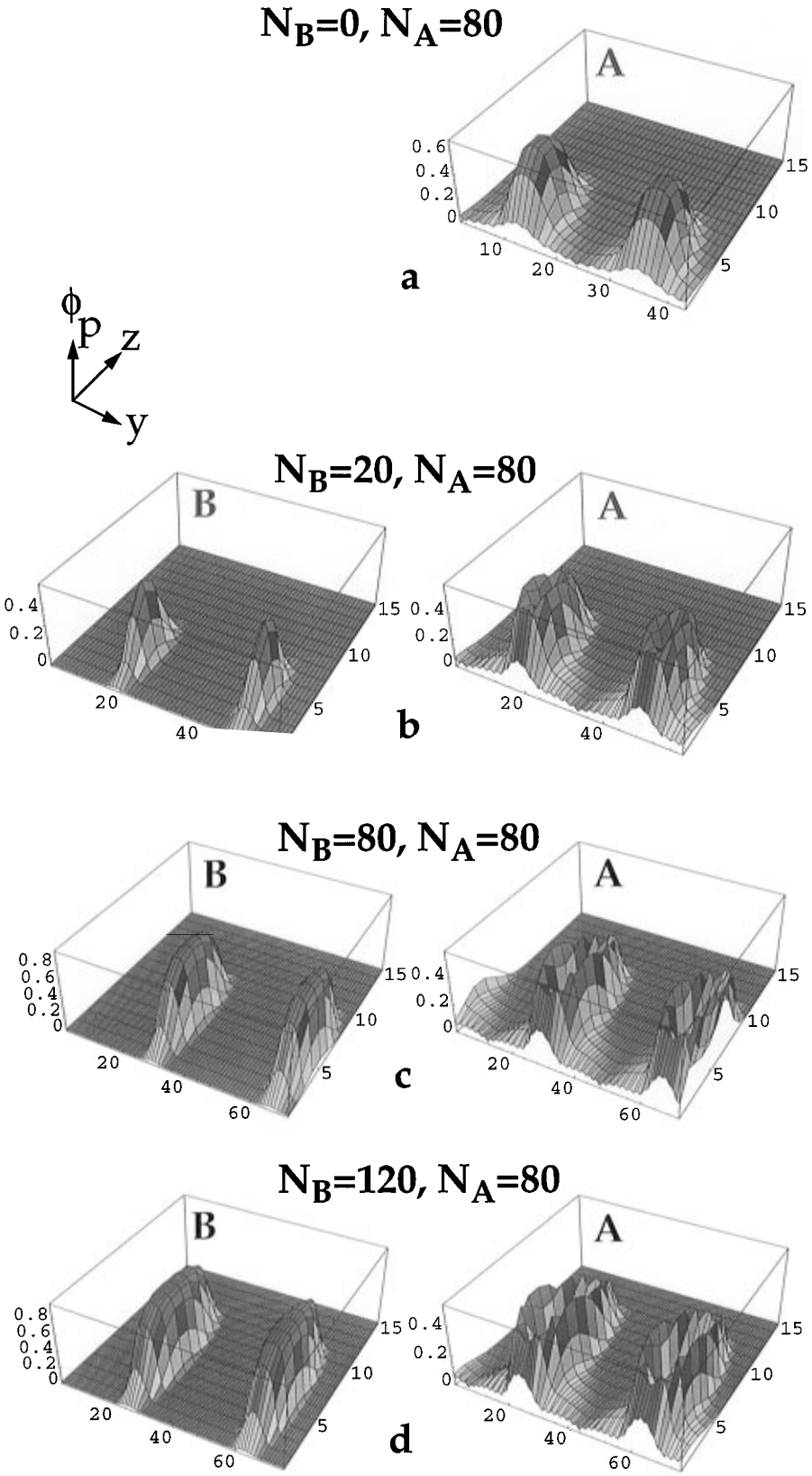

Figure 4. Results from the 2D SCF calculations. The plots reveal the effect of increasing N_B,while keeping N_A fixed at 80. The diblock copolymers are grafted by the more soluble A component The parameter N_B has the following values: (a) $N_B = 0$, (b) $N_B = 20$, (c) $N_B = 80$, and (d) $N_B = 120$. The other parameters are set at $\rho = 0.025$, $\chi_{BS} = 2$, $\chi_{AS} = 1$, and $\chi_{AB} = 0$. Y refers to the grafting direction, and ϕ_p denotes the polymer density. The plots marked B show the polymer density of the B blocks, while the plots marked A show the density of the A blocks.

becomes more extended as the size of the core increases with the increase in N_B.

Scaling Theory

To obtain a more quantitative description of these micellar onions, we use scaling theory to formulate an expression for the free energy of our system. To carry out this analysis, we first consider the behavior of a collapsed homopolymer in a poor solvent. The collapsed chain can be viewed as a spherical globule of radius $R \sim a(N/\tau)^{1/3}$, which is densely filled with thermal blobs

of the size $\xi \sim a/\tau$.[13,14] Within each blob, the chain obeys Gaussian statistics, i.e., a blob contains $n \sim \xi^2 \sim 1/\tau^2$ polymer units and the free energy per blob is on the order of $-kT$. The volume fraction of polymer units in the globule scales as $c \sim n/\xi^3 \sim \tau$. The surface tension γ between the boundary of the globule and the pure solvent can be estimated as $\gamma \sim kT/\xi^2$, i.e., it is the number of thermal blobs per unit area of the boundary. This implies that the width of the boundary is of the order of ξ and thus is small with respect to the total size of the globule R.

When two different components are linked together to form a diblock, the components segregate and each block forms a phase with concentrations $c_A \sim \tau_A$ and $c_B \sim \tau_B$, respectively. The entire copolymer adopts an "onion" conformation, where the less soluble component (B) forms the internal part of the globule, and the more soluble component (A) forms the outer, spherical coating. The inner, dense core has a radius R_B, whereas the total radius of the "onion" is $R \sim (N_A/\tau_A + N_B/\tau_B)^{1/3}$. As noted above, this conformation minimizes the surface tensions and thereby lowers the free energy of the system. Specifically, at $\chi_{AB} = 0$ the surface tension at the A/B boundary can be estimated as $\gamma_{AB} \sim \gamma_B - \gamma_A$, and the width of this boundary[15] is $d \sim a/(\tau_B - \tau_A)$. On the other hand, the surface tension at the outer boundary is still γ_A. In formulating this onion model, we assume that $d \ll R_B$ and $d \ll (R - R_B)$, i.e., that there is a noticeable difference between the A and B solubilities.

One could argue that the difference in solubilities and thus the surface tensions at the boundaries between polymer and solvent ($\gamma_A \sim \tau_A^2$, $\gamma_B \sim \tau_B^2$) could drive the system to form a "dumbbell" conformation, where the chains form two individual spherical globules with radii $R_A \sim a(N_A/\tau_A)^{1/3}$ and $R_B \sim a(N_B/\tau_B)^{1/3}$. Comparing the losses in the free energy at the boundaries for both the onion and the dumbbell conformations (see Figure 1c)

$$\Delta F_{surf} = \Delta F_{surf}^{\ dumbbell} - \Delta F_{surf}^{\ onion} = [\gamma_A R_A^{\ 2} + \gamma_B R_B^{\ 2}] - [\gamma_A R^2 + \gamma_{AB} R_B^{\ 2}] = \gamma_A[R_A^{\ 2} + R_B^{\ 2} - R^2] > 0 \quad (7)$$

we find that forming an onion is more favorable than splitting into a dumbbell. An increase in $\chi_{AB} > 0$ will lead to an increase in the surface tension between the A and B blocks and will eventually drive the onion to separate into a dumbbell. In this paper, however, we focus on the case of nearly compatible blocks.

At sparse grafting densities, individual diblocks will aggregate to form multichain onions (as evidenced by the SCF calculations). Furthermore, the overall layer forms multiple onions. If the surface is nonadsorbing, the chains will not wet the surface and the multichain onions remain roughly spherical in shape. In our scaling analysis, we assume that each onion is composed of a central core, which contains the inner B region and the outer A shell, and strongly stretched legs, which tether the core to the surface. For a core consisting of f chains, the radius R_B of the inner (denser) part scales as

$$R_B \sim a(N_B f/\tau_B)^{1/3} \quad (8)$$

whereas the total radius of the core R is given by

$$R \sim a(N_B f/\tau_B + N_A f/\tau_A)^{1/3} \quad (9)$$

The corresponding free energy of the core per chain is

$$\Delta F_{surf}/kT \sim [\gamma_A R^2 + (\gamma_B - \gamma_A) R_B^{\ 2}]/f \sim (\tau_B^{\ 4/3} N_B^{\ 2/3}/f^{1/3})[1 - (1/x^2) + (1 + xN_A/N_B)^{2/3}/x^2] \quad (10)$$

where $x = \tau_B/\tau_A > 1$.

The conformational losses due to the stretching of the legs depend on the type of block that is grafted onto the surface. As in the SCF studies, we consider both cases: chains tethered by the end of the more soluble block and those tethered by the less soluble component. To facilitate the scaling analysis, we first consider the case where the chains are grafted by A, the more soluble block (that is, $\tau_A < \tau_B$).

Chains Grafted by the More Soluble Block. Here, the legs are formed from component A and they are strings of thermal blobs of size $\xi_A \sim a/\tau_A$. Thus, the elastic free energy per leg is given by[1,8]

$$\Delta F_{el}/kT \sim \tau_A D \sim \tau_A (fs)^{1/2} \quad (11)$$

where $D^2 = fs$ is the total area of the pinned, micellar onion. The total free energy per chain is

$$\Delta F = \Delta F_{surf} + \Delta F_{el} \quad (12)$$

and minimizing this expression with respect to f gives

$$f \sim \tau_B^{\ 2/5} N_B^{\ 4/5} x^{6/5} s^{-3/5} [1 - (1/x^2) + (1 + xN_A/N_B)^{2/3}/x^2]^{6/5} \quad (13)$$

One can extract two different asymptotes from the eq 13. In the first limiting case, $N_A/(x^2 N_B) \gg 1$, and

$$f \sim \tau_A^{\ 2/5} N_A^{\ 4/5}/s^{3/5} \quad (14)$$

In the second limiting case, $N_A/(x^2 N_B) \ll 1$, the term in square brackets is of order unity, and one has

$$f \sim \tau_B^{\ 2/5} N_B^{\ 4/5} x^{6/5}/s^{3/5} \quad (15)$$

The first case, $N_A/(x^2 N_B) \gg 1$, corresponds to relatively long blocks of A, and the surface free energy of the core is dominated by the contribution from the outer shell, whereas the contribution from the inner (denser) core is relatively small. As a result, eq 14 is identical with the scaling relationship for a pinned micelle of pure A.[1,8] The presence of the B component manifests itself only through weak dependences of R, D, and f on N_B. Thus, we have

$$D \sim (fs)^{1/2} \sim a\tau_A^{\ 1/5} N_A^{\ 2/5} s^{1/5} \quad (16)$$

$$R \sim a(N_A f/\tau_A)^{1/3} \sim aN_A^{\ 3/5}/(\tau_A s)^{1/5} \quad (17)$$

The second case, $N_A/(x^2 N_B) \ll 1$, corresponds to long B blocks. Here, the surface free energy is mainly determined by the A/B boundary within the core, i.e., it is governed by the second component. On the other hand, the stretching of the legs is still given by eq 11. As a result, one gets the new dependence given in eq 15 for the number of chains in a micelle, where f now depends on N_B and x. Here

$$D \sim (fs)^{1/2} \sim a(\tau_B s)^{1/5} N_B^{\ 2/5} x^{3/5} \quad (18)$$

whereas the radius of the core $R \sim a(N_B f/\tau_B + N_A f/\tau_A)^{1/3}$

scales as

$$R \sim a(\tau_B s)^{-1/5} x^{11/15} N_A^{1/3} N_B^{4/15} \qquad xN_A/N_B \gg 1 \quad (19)$$

$$R \sim a(\tau_B s)^{-1/5} x^{2/5} N_B^{3/5} \qquad xN_A/N_B \ll 1 \quad (20)$$

It follows from eq 18 that in the second scenario, an increase in N_B leads to an increase in D, the size of the micelle, and the legs of the micelle ($\sim D$) become longer. When $D \sim aN_A\tau_A$, nearly all the A units go into making legs and the core of the micelle is now formed by the B's. Under these conditions, the core of the micelle can be viewed as a densely packed system of thermal blobs of size $\xi_B \sim a/\tau_B$, whereas the legs are the strings of thermal blobs of size $\xi_A \sim a/\tau_A$. Any further increase in N_B will cause a further increase in the length of the legs. If the blob sizes were equal, the length of the legs could be increased by pulling the B's from the core. However, the tension in the legs, $D/N_A \sim \tau_A$, is smaller than the critical tension τ_B necessary to extract units of the less soluble B. Thus, the only means of increasing the length of the legs is to stretch them further, i.e., destroy the internal structure of the thermal blobs. Since strongly stretched, collapsed chains obey Gaussian statistics,[16] the elastic free energy of the legs is now given by

$$\Delta F_{el}/kT \sim D/a^2 N_A \sim fs/a^2 N_A \quad (21)$$

Adding eq 21 to the surface free energy of a core composed of pure B:

$$\Delta F_{surf}/kT \sim \tau_B^{4/3} N_B^{2/3}/f^{1/3} \quad (22)$$

and minimizing the resulting expression with respect to f, one gets the novel dependence for the equilibrium number of chains in the micelle:

$$f \sim \tau_B N_B^{1/2} N_A^{3/4}/s^{3/4} \quad (23)$$

where f now depends on both N_A and N_B. Correspondingly

$$D \sim (fs)^{1/2} \sim a\tau_B^{1/2} s^{1/8} N_A^{3/8} N_B^{1/4} \quad (24)$$

$$R \sim a(fN_B/\tau_B)^{1/3} \sim aN_B^{1/2} N_A^{1/4} s^{-1/4} \quad (25)$$

The dependences in eqs 23−25 for f, D, and R are valid only in the limited range where the tension in the legs is $\tau_A < D/N_A < \tau_B$. At the upper boundary, $D \sim \tau_B N_A$, the tension in the legs becomes equal to the critical value necessary to extract B units from the globular core. Here, the legs can be viewed as stretched blobs of size $\xi_A \sim \xi_B \sim a/\tau_B$. Now, the elastic stretching of the legs is given by

$$\Delta F_{el}/kT \sim \tau_B D \sim \tau_B (fs)^{1/2} \quad (26)$$

Summing eqs 22 and 26 and minimizing with respect to f, we arrive at the familiar scaling dependences:

$$f \sim \tau_B^{2/5} N_B^{4/5}/s^{3/5} \quad (27)$$

$$D \sim (fs)^{1/2} \sim a(\tau_B s)^{1/5} N_B^{2/5} \quad (28)$$

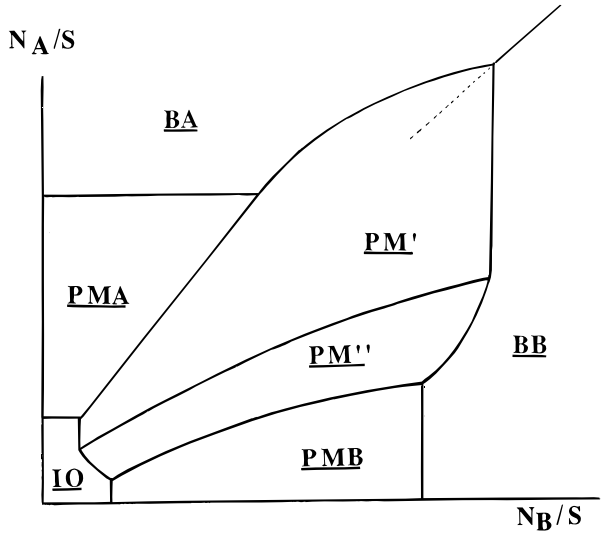

Figure 5. Diagram of states for a layer grafted by the more soluble A blocks. The coordinates of the plot are $u = N_A/s$ and $v = N_B/s$. The various regimes are discussed in the text.

$$R \sim a(fN_B/\tau_B)^{1/3} \sim a(\tau_B s)^{-1/5} N_B^{3/5} \quad (29)$$

corresponding to pinned micelles of pure B. (The A parts of the legs coexist with B parts at a fixed value of tension τ_B.)

Diagram of States. The above results are summarized in the diagram of states (Figure 5), plotted in the reduced coordinates $u = N_A/s$ and $v = N_B/s$. (To facilitate comparison between the diagram of states and the SCF results, we note that Figures 3 and 4 correspond to setting $u = N_A/s = 1$ and $v = N_B/s = 1$.) Regions PMA, PM′, PM″, and PMB correspond to the regimes of the pinned micellar onions discussed in the above section. In the PMA region, the A blocks are relatively long and the structure of the micelle is virtually the same as that for homopolymer micelles formed from pure A (see eqs 14, 16, and 17). In the PMB region, the A blocks are short compared to the B blocks, and the micellar structure coincides with that of a homopolymer micelle formed from pure B (see eqs 27−29). In the PM′ and PM″ regions, the structures of the micelle are affected by both block lengths since the legs are formed from A units and the core has an onionlike structure (region PM′, eqs 15, 18, and 19) or consists of pure B (region PM″, eqs 23−25). Here, the characteristics of the micelles are governed by the solubilities of both blocks (PM′, PM″), as well as by the molecular weights of the blocks (PM″). The boundaries between the various PM regimes can be found by equating the sizes of the micelles in any two neighboring regions.

One finds additional regimes IO and BA, BB in the diagram of Figure 5. The region of individual onions (IO) is found at small values of the grafting density. The boundaries between this regime and any of the PM regimes is determined by the condition $f \sim 1$. The regions BA and BB (brush regimes) correspond to dense grafting of the chains, where at least one of the components forms a continuous layer. In the BA regime, the continuous layer is always formed by the A component and N_A determines the overall thickness of the film, $H \sim H_A$, where

$$H_A \sim a^3 N_A/(\tau_A s) \quad (30)$$

In the BB regime, the B component forms the continuous layer with thickness

$$H_B \sim a^3 N_B/(\tau_B s) \tag{31}$$

and the overall brush thickness is given by $H \sim H_B$. The boundaries between the B and the PM regimes are found from the condition $D \sim R$, which corresponds to a merging of neighboring micelles. Finally, the boundary between the regimes BA and BB is found by setting $H_A \sim H_B$. It should be noted that in the regimes BA and BB, the discontinuous component can form micelle type structures. (Here, we do not consider the details of these structures.) However, at sufficiently long lengths for both blocks (deep in the regimes BA and BB), one expects the formation of two continuous layers, one on top of the other.

Chains Grafted by the Less Soluble Block. We now consider the opposite case, where the chains are grafted onto the surface by the less soluble B block. As predicted by the SCF calculations, this system is also expected to form pinned micellar onions. The core of the micelles will have an onionlike structure and, thus, the surface free energy per chain is still given by eq 10. The legs are now composed of B segments and their elasticity is given by eq 26. Adding equations 10 and 26 and minimizing with respect to f, one obtains the equilibrium number of chains within the structure:

$$f \sim (\tau_B^{2/5} N_B^{4/5}/s^{3/5})[1 - (1/x^2) + (1 + xN_A/N_B)^{2/3}/x^2]^{6/5} \tag{32}$$

As indicated by eq 10, for relatively short A blocks, or $N_A \ll x^2 N_B$, the surface free energy of the core is determined by the internal A/B boundary and scales according eq 26. Balancing eqs 22 and 26 (or neglecting the term in square brackets in eq 32), we arrive at the results in eqs 27−29, describing the pinned micelles formed by the pure B component. Thus, for short A blocks, the characteristics of the micelles are predominantly governed by the solubility parameter τ_B and the molecular weight N_B of the less soluble component and depend on N_A only through a weak, non-power-law dependence.

An increase in N_A, the length of the outer block, leads to a corresponding increase in the size of the core, as given by eq 9, at approximately fixed f. This increase in R leads, in turn, to an increase in the surface free energy associated with the external boundary:

$$\Delta F^A_{surf}/kT \sim \tau_A^{4/3} N_A^{2/3}/f^{1/3} \tag{33}$$

where f is still given by eq 27. Since f does not depend on N_A, eq 33 indicates that $\Delta F^A_{surf}/kT$ increases rapidly with N_A. To diminish the unfavorable contact with the solvent, the micelle has to rearrange its structure. In particular, the outer A component can form its own large micelles, in addition to covering the inner B core. This rearrangement occurs when the free energy per A block in an individual pinned micelle formed from pure A:

$$\Delta F^A/kT \sim \tau_A^{6/5} N_A^{2/5} s^{1/5} \tag{34}$$

becomes comparable to $\Delta F^A/kT$ in eq 33, i.e., at $N_A \sim x^{1/2} N_B$ where, as before, $x = \tau_B/\tau_A > 1$. Thus, at higher values of $N_A > x^{1/2} N_B$, one expects a splitting of the original onionlike micelles onto "garlics": smaller, multiple B cores are encircled by bigger A micelles, as shown in Figure 2d. The numbers of chains f_A and f_B in these

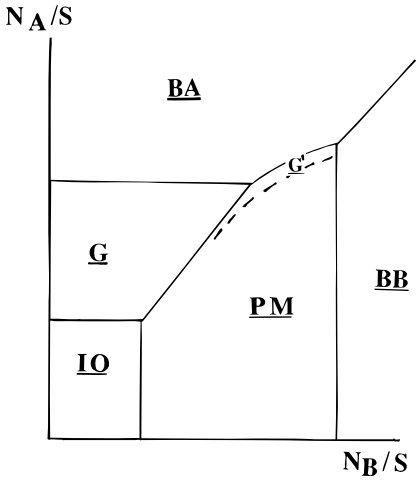

Figure 6. Diagram of states for a layer grafted by the less soluble B blocks. The coordinates of the plot are $u = N_A/s$ and $v = N_B/s$. The various regimes are discussed in the text.

micelles scale as

$$f_A \sim \tau_A^{2/5} N_A^{4/5}/s^{3/5} \tag{35}$$

$$f_B \sim \tau_B^{2/5} N_B^{4/5}/s^{3/5} \tag{36}$$

and, thus, one finds $f_A/f_B \sim N_A/(x^{1/2} N_B)^{4/5} > 1$ micelles of the B component per one micelle of the A component. The cores of smaller B micelles are coated by the outer A component where possible, and we call such structures "garlics" in order to emphasize the fact that the A coating contains spatially separated cores of the inner B component.

Diagram of States. The areas where the "onions" and "garlics" appear as stable structures are marked in the diagram of states, which is plotted as a function of the reduced coordinates $u = N_A/s$ and $v = N_B/s$ in Figure 6. (The appropriate SCF results, shown in Figure 2, correspond to setting $v = N_B/s = 1$.) In addition to the onions (PM) and garlics (G) regimes, the IO, BA, and BB regimes are also present in the diagram. As before, individual onions, IO, are found at sparse grafting densities. The brush regimes BA and BB, where at least one of the components forms a continuous layer, are found at high grafting densities.

The boundary between the BA and PM regimes has a complicated structure. In the vicinity of this boundary, the cores of the pinned micelles have an onionlike structure and are primarily composed of an outer A coating, with $R \sim a(N_A f/\tau_A)^{1/3}$. The periodicity of the system, however, $D \sim a(\tau_B s)^{1/5} N_B^{2/5}$ is mainly determined by the B block. An increase in N_A leads to an increase in $R \sim N_A^{1/3}$. At values of $R \sim D$ (near the PM/BA boundary), two neighboring cores will merge into one, larger core. This behavior diminishes the total external surface area and results in a gain in the surface free energy. As a result, two micelles form a garliclike structure: the cores of two neighboring micelles are coated by a common spherical shell of A. Figure 2d reveals the conformation of such garliclike structures. The difference between these structures (G′) and the garlics in region G is that within the G′ domain, the B blocks are sufficiently long that the A's do not contribute to forming legs. Further increases in N_A will lead to a further merging of the cores, forming higher order structures until the A component forms a continuous layer.

Adsorbed Pinned Micelles. In the above calculations, we assumed that the interaction of the blocks with the surface is the same as that with the solvent. We now allow the blocks to adsorb onto the grafting surface, and we determine how the polymer−surface interactions affect the conformation of the micellar structures. We assume that A and B units in direct contact with the surface experience an adsorption energy of δ_A and δ_B, respectively. Under the conditions of weak adsorption, where $\delta_A/kT \ll \tau_A$ and $\delta_B/kT \ll \tau_B$, the interactions with the surface do not destroy the internal structure of the thermal blobs, and in general, the partially spread core of the micelle retains its globular conformation. (The average concentration of units inside the core is determined by the solvent quality and the chains are locally Gaussian.) Interactions with the surface will, however, lead to a deformation of the core; the phenomenon is similar to that which occurs when a liquid droplet partially wets a surface.[17] The wetting of a grafting surface by pinned homopolymer micelles was recently considered in ref 6. Following the arguments in ref 6, we consider the wetting of the substrate by the onionlike micelles. We assume that both components A and B spread on the surface, conserving their internal polymer concentrations ($\sim\tau_A$ and $\sim\tau_B$), and the components are demixed, as in a totally nonwetting core. Under these conditions, each of the components can be envisioned as forming a spherical cap with a contact angle Θ. Introducing the surface tensions γ_{Aw}, γ_{Bw}, and γ at the respective A−wall (synonymous with surface), B−wall, and solvent−wall boundaries, we can apply Young's law to determine the equilibrium contact angles for both the components:

$$\cos \Theta_A = (\gamma - \gamma_{Aw}/\gamma_A) \tag{37}$$

$$\cos \Theta_B = (\gamma_{Aw} - \gamma_{Bw})/(\gamma_B - \gamma_A) \tag{38}$$

Within the blob model the values of the surface tensions γ_{Aw} and γ_{Bw} can be related to the values of the adsorption energies as[6,17]

$$(\gamma - \gamma_{iw}/\gamma_i) \sim \delta_i/\tau_i kT \qquad i = \text{A, B} \tag{39}$$

where $\delta_i > 0$ (<0) corresponds to an attractive (repulsive) interaction. After simple algebraic transformations similar to those in ref 6, we can represent the surface free energy of a partially spread core as

$$\Delta F_{surf}/kT = \Delta F^0{}_{surf}/kT g(\Theta_A,\Theta_B,N_A,N_B) \tag{40}$$

where

$$g(\Theta_A,\Theta_B,N_A,N_B) = [g_A(1 + xN_A/N_B)^{2/3} + g_B(x^2 - 1)]/[(1 + xN_A/N_B)^{2/3} + (x^2 - 1)] \tag{41}$$

and

$$g_i = (1 - \cos \Theta_i)^{2/3}(^1/_2 + {}^1/_4 \cos \Theta_i)^{1/3} \qquad i = \text{A, B} \tag{42}$$

Here $\Delta F^0{}_{surf}/kT$ is the surface free energy of a totally dewetting core given by eq 10.

As can be seen from eqs 40 and 41, the partial spreading of the onion is accounted for by $g < 1$. As follows from eq 41, the adsorption of the core decreases the equilibrium size of the micelles. This effect is qualitatively similar to that predicted for homopolymer-pinned micelles.[6] It should be noted that the validity of the above equations is restricted by few conditions. In particular, we assume the "double-cap" structure of the adsorbed core, i.e., the outer A block should be long enough to provide a coating of the inner B. We also consider the case of weak adsorption. At high adsorption energies, leading to the destruction of the internal structure of thermal blobs, one expects wetting of the surface and the disappearance of onionlike micelles.

Discussion and Conclusions

To summarize, we used both SCF calculations and scaling arguments to demonstrate that grafted diblock copolymers exhibit a variety of structures in poor solvents. The detailed morphology of these structures depends on the solubility of the different blocks, the composition of the block copolymer and the manner in which the chains are grafted onto the surface (that is, whether they are tethered by the more or the less soluble block). Novel structures include onion- and garliclike pinned micelles. In particular, when the chains are grafted by the less soluble B block, and the grafting density is sufficiently low that the polymers do not interact, the diblocks associate into single-chain onions, with a B core and outer A layer. When the grafting density is increased to values near the overlap threshold, the copolymers associate into multichain onions. By increasing N_A relative to N_B at low grafting densities, the copolymers are driven to aggregate into single-chain or multichain garlics, where multiple B cores are covered by a continuous A layer. When the grafting density is relatively low and the chains are grafted by the A block, the copolymers can again form single-chain or multichain onions. As Figure 5 indicates, the exact morphology of the onions depends on the relative lengths and solubilities of the A and B blocks. On the other hand, grafting by the A block eliminates the garlics from this phase diagram; garlics are observed only when the copolymers are tethered by the less soluble B block.

Whether the chains are grafted by the A or B blocks, increasing the grafting density significantly beyond the overlap threshold ultimately causes one or both components to form a continuous layer. For long blocks and high grafting densities, the layer eventually forms a laterally homogeneous brush.

The above calculations were carried out for the case of compatible blocks ($\chi_{AB} = 0$). An increase in χ_{AB} will result in the segregation of the A and B components and a subsequent splitting of the onionlike structure. In particular, when the chains are grafted by the less soluble B blocks, the chains can form dumbbell-like structures, where the B core lies near the surface and an A micelle sits atop the B domain. Such A and B pinned micelles can coexist since the tension in the legs of the upper row of micelles ($\sim\tau_A$) is insufficient to destroy the micellar cores in the lower row. The shape of the cores may, however, be deformed. The details of such structural rearrangements within the dumbbell-like micelles are beyond the scope of this paper.

In the case where the chains are tethered by the more soluble A blocks, the copolymers cannot form such structures. Here, the tension in the B legs ($\sim\tau_B$) is greater than the force needed to extract A monomers from the core of the A micelles. As a result, A micelles are not formed; rather, the A segments contribute to the legs of the B micelles and also contribute to shielding the B core.

We note that if the grafting is relatively uniform, the micelles will form an ordered array or pattern on the surface. The advantage of forming patterned films with tethered copolymers is that the size and spacing of the micelles, and thus the dimensions of the pattern, can be controlled by varying the chain length, solvent quality, or grafting density. With the ability to control the size of the patterns, the films can be tailored for specific applications, including coatings for optoelectronic devices.

Acknowledgment. A.C.B gratefully acknowledges financial support from the Materials Research Center, funded by AFOSR, through Grant F49620-95-1-0167, and the DOE for financial support through Grant DE-FG02-90ER45438. C.S. also gratefully acknowledges financial support from NSF Grant DMR-92-17935 to D. M. Jasnow.

References and Notes

(1) Klushin, L. I., preprint, 1992.
(2) Williams, D. R. M. *J. Phys. II* **1993**, *3*, 1313.
(3) (a) Lai, P; Binder, K. *J. Chem. Phys.* **1992**, *97*, 586. (b) Yeung, C.; Balazs, A. C.; Jasnow, D. *Macromolecules* **1993**, *26*, 1914. (c) Grest, G. S.; Murat, M. *Macromolecules* **1993**, *26*, 3108. (d) Soga, K. G.; Guo, H.; Zuckermann, M. J. *Europhys. Lett.* **1995**, *29*, 531. (e) Stamouli, A.; Pelletier, E.; Koutsos, V.; Vegte, E. van der; Hadziioannou, G. *Langmuir*, in press.
(4) Siqueira, D. F.; Kohler, K.; Stamm, M. *Langmuir* **1995**, *11*, 3092.
(5) Singh, C.; Balazs, A. C. *J. Chem. Phys.*, in press.
(6) Singh, C.; Zhulina, E. B.; Gersappe, D.; Pickett, G. T.; Balazs, A. C. *Macromolecules*, submitted.
(7) Zhulina, E. B.; Balazs, A. C. *Macromolecules* **1996**, *29*, 2667.
(8) Zhulina, E. B.; Birshtein, T. M.; Priamitsyn, V. A.; Klushin, L. I. *Macromolecules* **1995**, *28*, 8612.
(9) Dong, H. *J. Phys. II* **1993**, *3*, 999.
(10) Soga, K. G.; Zuckermann, M., J.; Guo, H. *Macromolecules* **1996**, *29*, 1998.
(11) Marko, J. F.; Witten, T. A. *Macromolecules* **1992**, *25*, 296.
(12) Fleer, G. J.; Cohen Stuart, M. A.; Scheutjens, J. M. H. M.; Cosgrove, T.; Vincent, B. *Polymers at Interfaces*; Chapman and Hall: London, 1993.
(13) Lifshitz, I. M.; Grosberg, A. Y.; Khokhlov, A. R. *Rev. Mod. Phys.* **1978**, *50*, 6831.
(14) Williams, C.; Brochard, F.; Frisch, H. L. *Annu. Rev. Phys. Chem.* **1981**, *32*, 433.
(15) Noolandi, J.; Hong, K. M. *Macromolecules* **1983**, *16*, 1443.
(16) Halperin, A.; Zhulina, E. B. *Europhys. Lett.* **1991**, *15*, 417.
(17) Johner, A.; Joanny, J. F. *J. Phys. II* **1991**, *1*, 181.

MA960498I